International Journal of Minerals, Metallurgy and Materials
Volume 27, Number 1, January 2020, Page 1
https://doi.org/10.1007/s12613-019-1939-x

Invited Review

Recent progress in third-generation low alloy steels developed under M^3 microstructure control

Zhen-jia Xie[1), *Cheng-jia Shang*[1), *Xue-lin Wang*[1), *Xue-min Wang*[1), *Gang Han*[2),
and Raja-devesh-kumar Misra[3)

1) Collaborative Innovation Center of Steel Technology, University of Science and Technology Beijing, Beijing 100083, China
2) Institute of Advanced Materials and Technology, University of Science and Technology Beijing, Beijing 100083, China
3) Laboratory for Excellence in Advanced Steel Research, Department of Metallurgical, Materials and Biomedical Engineering, University of Texas at El Paso, El Paso, TX 79968, USA

(Received: 5 July 2019; revised: 31 October 2019; accepted: 1 November 2019)

Abstract: During the past thirty years, two generations of low alloy steels (ferrite/pearlite followed by bainite/martensite) have been developed and widely used in structural applications. The third-generation of low alloy steels is expected to achieve high strength and improved ductility and toughness, while satisfying the new demands for weight reduction, greenness, and safety. This paper reviews recent progress in the development of third-generation low alloy steels with an M^3 microstructure, namely, microstructures with multi-phase, meta-stable austenite, and multi-scale precipitates. The review summarizes the alloy designs and processing routes of microstructure control, and the mechanical properties of the alloys. The stabilization of retained austenite in low alloy steels is especially emphasized. Multi-scale nano-precipitates, including carbides of microalloying elements and Cu-rich precipitates obtained in third-generation low alloy steels, are then introduced. The structure–property relationships of third-generation alloys are also discussed. Finally, the promises and challenges to future applications are explored.

Keywords: third-generation low alloy steels; multi-phase microstructure; meta-stable retained austenite; multi-scale precipitates

1. Introduction

Low alloy steels deliver high performance at low economical cost. Therefore, they are widely used in structures such as high buildings, marine formations, bridges, and ships [1–5]. Within the past 20–30 years, the commercial steel market in China has been dominated by ferrite/pearlite dual-phase steels (first-generation steels) and bainitic or martensitic steels (second-generation steels) [6]. However, both types of steels are limited by their microstructures. First-generation steels are highly ductile but their yield strength is low, whereas second-generation steels achieve high yield strength but are disadvantaged by high yield ratio and poor ductility or weldability. The increase in architectural facilities, rapid development of equipment, and strong emphasis on environmental protection has necessitated the development of structural steels with higher strength and better ductility and toughness (third-generation steels) than the existing steels. Such developments aim to maintain structural safety while saving raw material resources [7].

In 2010, the National Basic Research Program of China (the 973 Program) launched a research project on the third phase of new-generation steels. The control of microstructures with multi-phase, meta-stable, and multi-scale (M^3) was proposed as a novel concept by Dong *et al.* [7]. Such prototype technologies might obtain steels with high comprehensive performance, such as third-generation low alloy structural steels, third-generation automotive sheet steels, and third-generation heat-resistant martensitic steels. In third-generation automotive sheet steels, high plasticity can be achieved by retaining a large amount of meta-stable austenite in the multi-phase microstructure. In fact, austenite is composed of multi-scale-sized grains with different stabilities. Therefore, the M^3 microstructure usually refers to a multi-phase micro-

---

Corresponding author: Cheng-jia Shang E-mail: cjshang@ustb.edu.cn structure of meta-stable retained austenite having a multi-scale grain size.

Recent studies on advanced steels commonly aim to obtain multi-phase microstructures containing significant amounts of retained austenite with controllable stability. For this purpose, the chemical composition must contain austenite-stabilizing alloying elements, and the heat treatment should favor a multi-phase microstructure, and stabilize the untransformed austenite during the cooling process. These requirements have been met by transformation-induced plasticity (TRIP) [8–9], quenching, and partitioning (Q&P) [10–11], annealing reverted transformation (ART) [12–13], and twinning induced plasticity (TWIP) [14–15]. In TRIP and Q&P steels, the austenite is stabilized by diffusion of carbon from bainite or as-quenched martensite during the austempering or partitioning process, whereas in ART steels, it is stabilized by enrichment with manganese in the reversed austenite during intercritical annealing. The microstructure of TWIP steels is single-phase austenite with high manganese content. From the above discussion, it appears that high carbon or manganese content is needed to stabilize retained austenite. Obviously, this is undesirable for casting and welding.

Shang and colleagues proposed the multi-step intercritical process [16–17], a novel method that improves the comprehensive properties of steel. This method combines M^3 microstructures in third-generation low alloy steels to improve their strength, ductility, and low-temperature toughness. As cyclic heat treatments are carried out at high temperatures, multi-scale precipitation is necessary for achieving high strength via grain refinement, and precipitation strengthening. Hence, the M^3 microstructure of third-generation low alloy structural steels usually possesses a multi-phase microstructure, meta-stable retained austenite, and multi-scale precipitates.

This paper reviews the developmental progress of third-generation low alloy structural steels from several perspectives. First, it summarizes the relationship between the microstructure, and mechanical properties of the steels, focusing on control of the M^3 microstructure, especially by stabilizing the retained austenite. Next, it explores the potential applications and challenges that will motivate the future development of third-generation low alloy structural steels.

2. Alloy design and technical route

2.1. Alloy design

When designing the high strength low alloy steels for structural applications, weldability is of primary importance. To ensure good welding performance, the carbon equivalent (C_{eq}), and cold crack sensitivity (P_{cm}) should be as low as possible, which restricts the carbon and manganese contents. However, meta-stable retained austenite requires moderate amounts of austenite stabilizers (C, Mn, and Ni). To balance these opposing requirements, the combined amount of the added Mn and Ni does not exceed ~3wt%, with a carbon content less than 0.1wt%. For cost-effectiveness, the Ni additive is less than 1.0wt%. Other alloying elements (Nb, Cu, V, and Mo) are added to different strength grades. Hence, the prototypal chemical composition of low alloy structural steels with the M^3-type microstructure is 0.08wt%–0.1wt% C, 2.0wt%–2.5wt% Mn, 0.3wt%–0.8wt% Si, 0.5wt%–1.0wt% Ni, 0.5wt%–2.0wt% Cu, and 0.5wt% Mo+Nb+Ti+V.

2.2. Control route of the M^3 microstructure

Recently, the M^3 microstructure in low-carbon low alloy steels has been formed by a novel multi-step treatment. The multi-step processing and microstructural evolution is schematized in Fig. 1. The multi-step processing consists of three procedures. The first step is quenching after controlled rolling or full austenitization, which disperses the fine microalloying element carbides precipitated in the austenite, forming bainite/martensite with a high density of dislocations. Therefore, quenching obtains a bainite/martensite fine microstructure. Second, the quenched initial bainite/martensite is reheated to high temperature in the two-phase region for intercritical annealing, which forms reverted austenite. During the austenite reversion transformation, the austenite stabilizers such as C and Mn partition into reverted austenite. The resulting alloy is pre-enriched in reverted austenite, and transforms into martensite during subsequent cooling to room temperature. The un-reverted structure becomes intercritical ferrite due to its lean alloy and the recovery effect. Some of the dislocations are pinned by fine carbides and remain in the intercritical ferrite. Finally, the dual-phase microstructure is tempered near the Ac_1 temperature, defined as the lowest temperature, at which austenite can form at a given heating rate. In this process, called intercritical tempering, fine austenite reverts from alloy-rich martensite, and is further enriched by partitioning. Hence, meta-stable austenite can be retained at room temperature. Nano-sized microalloying element carbides and copper continue to precipitate during this step.

3. Mechanical properties

The mechanical properties, yield strengths and elongations of different generations of low alloy steels have been

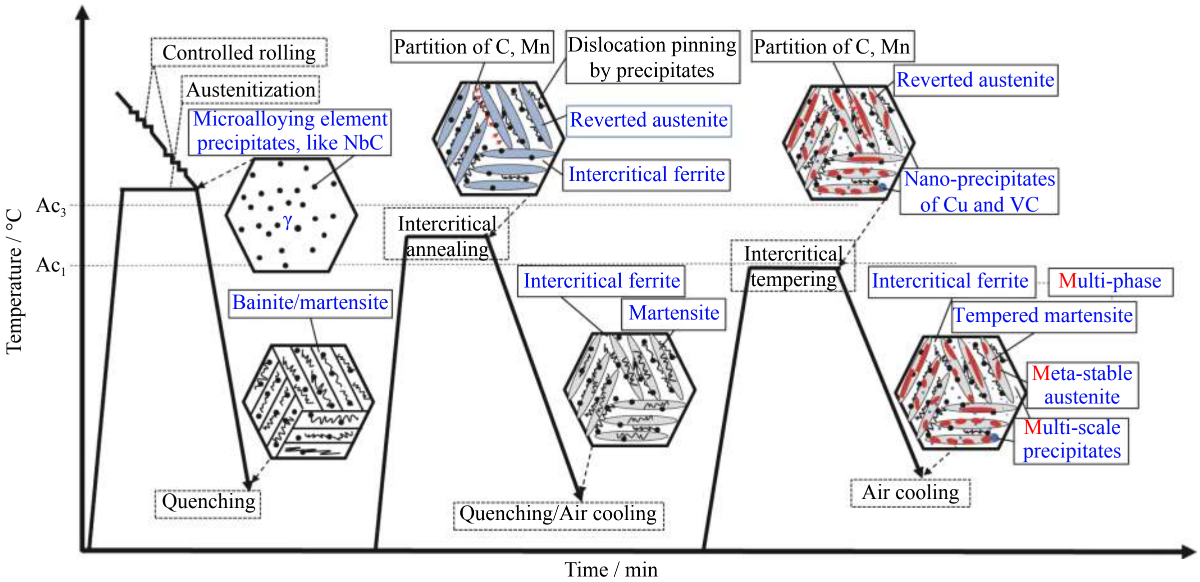

Fig. 1. Schematic of multi-step processing and microstructure evolution.

documented in the literatures [7,16–23], and are summarized in Fig. 2(a). First-generation low alloy steels have low yield strengths (295–460 MPa) and relatively high total elongations (20%–40%); conversely, second-generation low alloy steels have relatively high yield strength (500–1000 MPa) but poor ductility. However, third-generation low alloy steels simultaneously achieve high yield strength (500–800 MPa) and excellent ductility, with a total elongation similar to that of first-generation low alloy steels. Surprisingly, the uniform elongation of third-generation low alloy steels is 10%–25%, similar to the total elongation of second-generation low alloy steels. The high ductility is believed to be related to the increased work hardening rate caused by the austenite-to-martensite transformation during deformation (the TRIP effect). In conventional low alloy steels with single bainite, the work hardening rate decreases dramatically under stain. Ferrite in multi-phase pipeline steels can flatten the slope of decline [24]. However, third-generation low alloy steels present a three-stage work hardening behavior similar to that of medium-manganese steels with large amounts of retained austenite [25]. The work hardening initially decreases, then increases and maintains its high value until fracture. The increased work hardening rate is attributable to the TRIP effect.

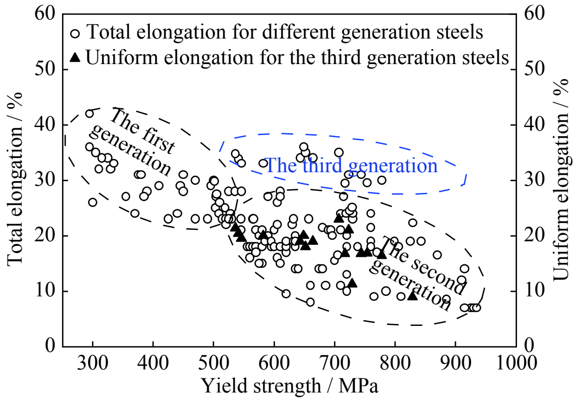

Fig. 2. Total elongation vs. yield strength of different generation low alloy structural steels and uniform elongation vs. yield strength of third-generation low alloy structural steels (for comparison).

Meta-stable retained austenite with high stability improves the impact toughness of third-generation low alloy steels with the M^3 microstructure [19,26]. Furthermore, the impact toughness is improved at low test temperatures, achieving a ductile-to-brittle transition temperature (DBTT) below −80°C. It is commonly recognized that highly stable meta-stable retained austenite enhances the toughness of steels. The role of the retained austenite has been variously speculated as scavenging harmful-elements [27], blocking crack [28], and absorbing additional energy via the martensitic transformation during fracture [29]. However, the toughness-enhancement mechanism of the retained austenite remains unclear, and may vary in different alloy systems. Preliminary studies [19,26] of third-generation low alloy steel suggested that under impact tests at lower temperature, the retained austenite enhances the plasticity before crack initiation. The enhanced plasticity not only increases the energy absorption before cracking, but also promotes beneficial dimple formation during cracking. Obviously, the amount of retained austenite and the low-temperature stability are crucial for improving the toughness of new-generation low alloy steels. This topic is worthy of future investigation.

4. Microstructural characteristics

4.1. Multi-phase microstructure with meta-stable retained austenite

Fig. 3(a) is a representative scanning electron microscopy (SEM) image of third-generation low alloy steel. Such steels have a refined multi-phase microstructure composed of intercritical ferrite, and tempered bainite/martensite. After intercritical annealing in the two-phase region, the austenite reversed from the initial bainitic/martensitic microstructure is uniformly distributed along the prior grain boundaries and lath boundaries. During austenite reversion, austenite stabilizers such as carbon and manganese in the un-reverted matrix are partitioned into austenite. After annealing, the alloying elements are depleted in the un-reverted matrix and form intercritical ferrite. The morphology of this intercritical ferrite (lath-like or granular) thus depends on the initial microstructure (lath bainite or granular bainite, respectively). Tempered bainite/martensite and retained austenite are uniformly dispersed within the ferritic matrix. The distribution and morphology of the retained austenite are revealed in the electron back scattering diffraction (EBSD) images, as seen in Fig. 3(b). The retained austenite is small-grained (less than 1 μm in size), and presents as a film-like structure between the matrix laths and a blocky structure at the boundary intersections. In X-ray diffraction analyses, the volume fraction of retained austenite in third-generation low alloy steels was determined as ~8%–26% [16–19,26,30]. It is worth noting that stabilizing the retained austenite is critically important in third-generation low alloy steels, but is not attempted in traditional multi-phase steels [31–32].

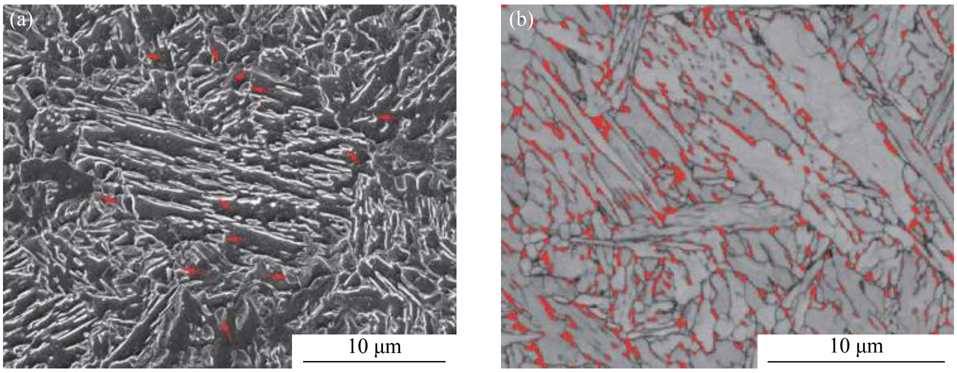

Fig. 3. Representative scanning electron microscopy (SEM) (a) and electron back scattering diffraction (EBSD) (b) images of the multi-phase microstructure of third-generation low alloy steels. The retained austenite is indicated by red arrows in (a) and the red areas in (b).

4.2. Stabilization of retained austenite

While some film-like austenite can remain in conventional low alloy steel [33], obtaining significant amounts of meta-stable retained austenite is a challenging task. In TRIP and Q&P steels with relatively high carbon content, the austenite is stably retained by the carbon enrichment [34–35]. In cryogenic steels with high Ni content, the retained austenite is stabilized by the nickel enrichment during tempering [36–39]. Recently, manganese enrichment of reverted austenite during intercritical annealing was reported to stabilize the austenite in medium-level manganese steels [40–42]. The retained austenite in new-generation low alloy steels is also enriched by manganese and nickel [19]. In further quantitative analyses, the manganese, and nickel contents that retained the austenite in third-generation steels were determined as ~6.8wt% and ~0.8wt%, respectively. As carbon is a very important austenite stabilizer with high diffusivity, it will likely be enriched in reverted austenite. To retain the austenite, a combined partitioning of C, Mn, and Ni has been tried in reverted austenite. The carbon concentration was lower in the retained austenite than in conventional TRIP or Q&P steels, and was determined as ~0.4wt% by atom probe tomography [43]. Clearly, large-size austenite alloyed 0.4C–6.8Mn–0.8Ni (wt%) cannot be stabilized at room temperature. For ultrafine grained austenite (<1 μm), martensitic transformation might require a large chemical driving force [44–45]. In addition, the martensite start temperature decreases with decreasing grain size of austenite [46–47]. These observations suggest that finely grained reverted austenite plays an important role in stabilizing austenite in third-generation low alloy steels at room temperature [44–45]. However, the stability of retained austenite is influenced by many complicated factors, including the chemical composition, morphology, surrounding matrix, size, and orientation. Therefore, the exact stabilization mechanism of austenite retention in third-generation low alloy steels remains unknown, and requires continuous efforts in future.

4.3. Multi-scale nano-precipitates

Along with multi-phase microstructures and meta-stable retained austenite, multi-scale precipitates determine the strength of third-generation low alloy steels. In third-generation low alloy steels, multi-scale precipitates are usually obtained by adding microalloying elements (such as titanium, niobium and vanadium), and copper. Representative precipitates obtained at different steps are presented in Fig. 4. After intercritical annealing, large rectangular particles of diameter ~10–30 nm and small spherical precipitates with diameters smaller than 10 nm are dispersed through the matrix, as shown in Fig. 4(a). In energy dispersive X-ray spectroscopy analyses, all precipitates were enriched in Nb, and some large and small precipitates contained Ti and Mo, respectively. The larger precipitates were (Nb,Ti)C composite carbides or Nb(C,N) carbonitrides formed at higher temperatures during the controlled rolling process. The nano-precipitates mainly contributed to the prior austenite grain refinement. The smaller (Nb,Mo)C or NbC precipitates were formed during inter-

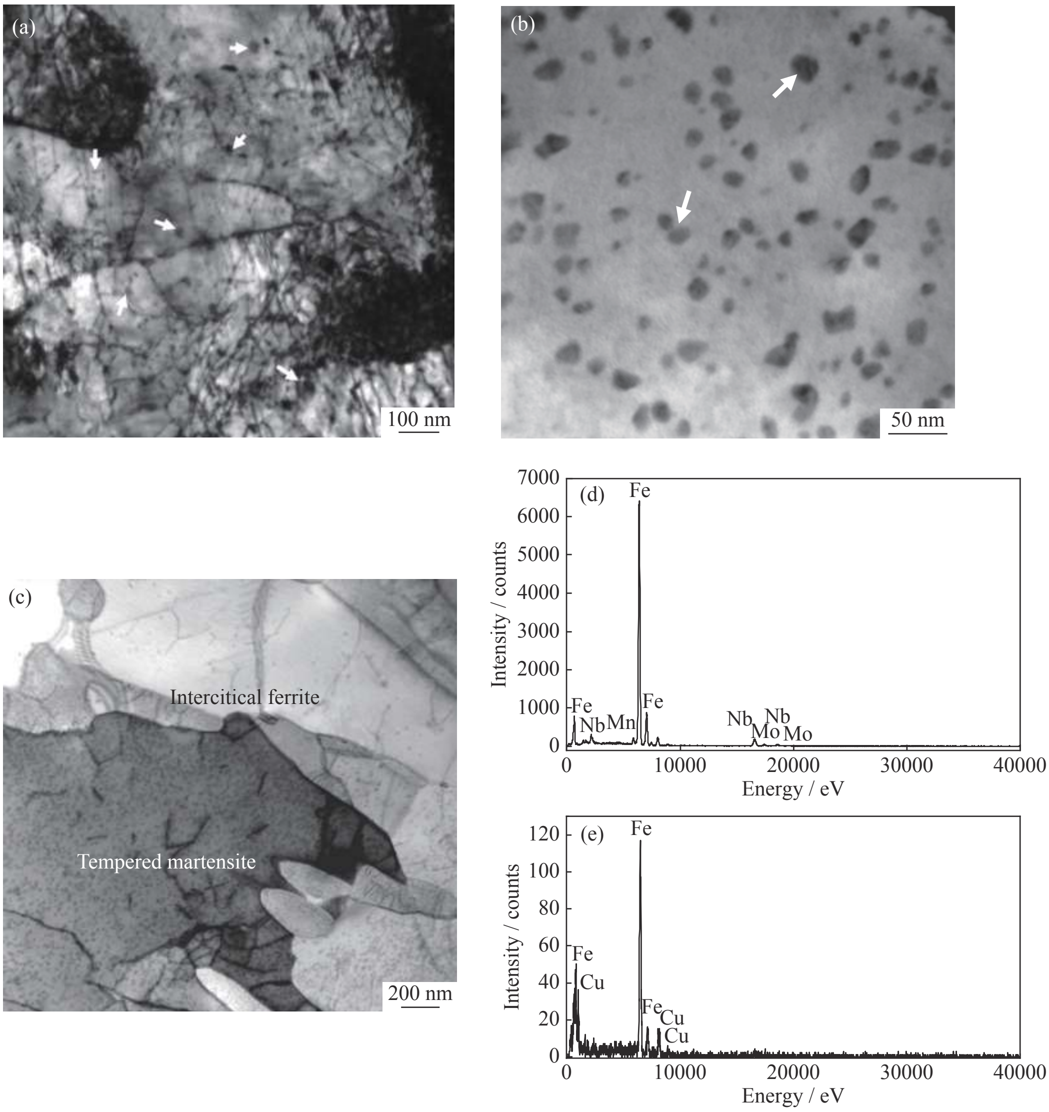

Fig. 4. TEM images of multi-scale precipitates obtained in different processing steps of third-generation low alloy steels: (a) nano-sized Nb-containing particles formed after intercritical annealing, (b) copper-rich precipitates formed after intercritical tempering, and (c) precipitation of copper-rich particles formed by additional tempering at 500°C; (d, e) typical spectra of (Nb,Mo)C precipitates in (a) and Cu precipitation in (b).

critical annealing; their smaller size was attributed to their precipitation at lower temperature than the controlled rolling temperature [48]. Notably, high density dislocations appeared in the annealed matrix, as seen in Fig. 4(a). One may reasonably conclude that these dislocations were pinned by the nano-sized (Nb,Mo)C or NbC. The pinning effect enhanced the yield strength by minimizing the strength loss during the recovery and new ferrite formation stages. Intercritical tempering yielded both Nb-containing precipitates and copper-rich precipitates as seen in Fig. 4(b). The copper-rich precipitates were spherical with diameters of ~5–20 nm. Copper precipitates at lower temperature than other microalloying elements because it is highly soluble in the body-centered cubic (bcc) matrix. Copper precipitation begins at ~680°C and peaks at ~500°C. Therefore, additional tempering at ~500°C facilitates the continuation of nano-sized copper-rich precipitation, as shown in Fig. 4(c). Note that the copper-rich precipitation is in homogeneously distributed through the bcc matrix. The enhanced density of copper-rich precipitate in tempered martensite implies that copper also partitions into reverted austenite by intercritical annealing, increasing the copper content of the martensitic phase in the dual-phase microstructure. Moreover, copper-rich precipitates in the retained austenite were observed after additional tempering at 500°C [18]. Copper-rich precipitation strengthens the hard phase of both the tempered martensite and the martensite newly formed from the meta-stable austenite in the multi-phase microstructure. Thus, precipitation in the retained austenite and the in homogeneously distributed copper-rich precipitates in the bcc matrix enhance the tensile strength of the steel. The tensile strength of multi-phase microstructure steels is mainly determined from the strength and volume fraction of the hard phase. Copper-rich precipitation selectively precipitated in meta-stable asutenite and hard tempered martensite is a promising alternative approach for reducing the yield ratio. Overall, the multi-scale nano-precipitates improve the yield strength of third-generation low alloy steels.

5. Future prospects and challenges

The strength of conventional low alloy steels is generally enhanced by inducing high dislocations and nano-sized precipitation. However, these techniques little enhance the ductility, and may actually degrade the toughness. Because precipitation strengthening and dislocation hardening increase the yield strength without enhancing the fracture stress, they decrease the plastic zone of crack tips [49–50]. Meta-stable retained austenite combined with multi-phase and multi-scale precipitation (the M^3 microstructure) significantly enhances the strength, ductility, and toughness of third-generation low alloy steels; especially, it improves the low- temperature toughness and decreases the DBTT. Therefore, third-generation low alloy steels with the M^3 microstructure are potentially available for tough applications such as seismic territories, low-temperature deep sea and polar regions, and large-scale structures (long-span bridges, ultra-large container ships, and marine engineering structures). In addition, the multi-phase, meta-stable, and multi-scale nature of the M^3 microstructure may be exploited in other materials.

Prior to applications, third-generation low alloy steels must overcome several problems. The main concern is the stability of meta-stable retained austenite in services. Owing to the meta-stable retention, the steels are vulnerable to low-temperature aging, fatigue, and welding and hydrogen embrittlement. An early study on 300 grade maraging steel indicated that the retained austenite increases the steel toughness, but does not significantly raise the fatigue strength [51]. Recent studies on bainitic steel [52] and quenching–partitioning–tempering steel [53] suggested that retained austenite improves the fatigue performance by blunting fatigue crack propagation and enhancing the plasticity near the tips of fatigue cracks. As the stability of the retained austenite dominates the fatigue performance, it must be prioritized in future investigations of third-generation low alloy steels. The other large challenge, improving the weldability, has been tackled in several studies. One promising solution is a newly designed weld metal with the optimum combination of alloying elements (1.5wt%–2.0wt% Mn, 0.9wt%–1.2wt% Ni, and 0.2wt%–0.25% Mo) and a suitably adjusted inter-pass temperature during multi-pass welding [54–56]. Moreover, the comprehensive performance of the base material and weld metal can be improved significantly by producing meta-stable retained austenite via an appropriate post-weld heat treatment [57–58]. This process has already produced hot bending pipes for deep sea applications [59].

6. Concluding remarks

Multi-step intercritical heat treatment is a novel method combining a multi-phase microstructure, meta-stable retained austenite, and multi-scale precipitates in low alloy systems. The microstructure is composed of intercritical ferrite, retained austenite, and tempered bainite/martensite. The combined effects of TRIP and precipitation strengthening boost the yield strength of low alloy steels to 500–800 MPa, while providing excellent ductility with a uniform elongation of 10%–25% and a total elongation exceeding 30%.

Meta-stable retention of austenite in the low alloy steel improves the impact toughness; especially, it decreases the DBTT of the steel. Third-generation low alloy steels with the M^3 microstructure are potentially applicable to high strength structures in seismic areas, long-span bridges, ship building, and marine engineering. Currently, these applications are precluded by several challenges, such as fatigue, weldability, and hydrogen embrittlement, which must be overcome in future investigation.

Acknowledgements

This work was financially supported by the National Natural Science Foundation of China (No. 51701012), the National Basic Research Program of China (973 Program: No. 2010CB630801) and the Fundamental Research Funds for the Central Universities (No. FRF-TP-17-004A1). R.D.K. Misra acknowledges continued collaboration with the University of Science and Technology Beijing as Honorary Professor.

References

[1] H.L. Fan, A.M. Zhao, Q.C. Li, H. Guo, and J.G. He, Effects of ausforming strain on bainite transformation in nanostructured bainite steel, *Int. J. Miner. Metall. Mater.*, 24(2017), No. 3, p. 264.

[2] B. Avishan, Effect of prolonged isothermal heat treatment on the mechanical behavior of advanced NANOBAIN steel, *Int. J. Miner. Metall. Mater.*, 24(2017), No. 9, p. 1010.

[3] S.G. Hashemi and B. Eghbali, Analysis of the formation conditions and characteristics of interphase and random vanadium precipitation in a low-carbon steel during isothermal heat treatment, *Int. J. Miner. Metall. Mater.*, 25(2018), No. 3, p. 339.

[4] D.L. Li, G.Q. Fu, M.Y. Zhu, Q. Li, and C.X. Yin, Effect of Ni on the corrosion resistance of bridge steel in a simulated hot and humid coastal-industrial atmosphere, *Int. J. Miner. Metall. Mater.*, 25(2018), No. 3, p. 325.

[5] B. Shahriari, R. Vafaei, E.M. Sharifi, and K. Farmanesh, Aging behavior of a copper-bearing high-strength low-carbon steel, *Int. J. Miner. Metall. Mater.*, 25(2018), No. 4, p. 429.

[6] Y.Q. Weng, C.J. Shang, and C.F. Yan, State-of-the-art and development trends of HSLA steels in China, *Iron Steel*, 46(2011), No. 9, p. 1.

[7] H. Dong, M.Q. Wang, and Y.Q. Weng, Performance improvement of steels through M^3 structure control, *Iron Steel*, 45(2010), No. 7, p. 1.

[8] Y.F. Shen, Y.D. Liu, X. Sun, Y.D. Wang, L. Zuo, and R.D.K. Misra, Improved ductility of a transformation-induced-plasticity steel by nanoscale austenite lamellae, *Mater. Sci. Eng. A*, 583(2013), p. 1.

[9] P.J. Jacques, Transformation-induced plasticity for high strength formable steels, *Curr. Opin. Solid State Mater. Sci.*, 8(2004), No. 3-4, p. 259.

[10] J.G. Speer, D.V. Edmonds, F.C. Rizzo, and D.K. Matlock, Partitioning of carbon from supersaturated plates of ferrite, with application to steel processing and fundamentals of the bainite transformation, *Curr. Opin. Solid State. Mater. Sci.*, 8(2004), No. 3-4, p. 219.

[11] J. Speer, D.K. Matlock, B.C. De Cooman, and J.G. Schroth, Carbon partitioning into austenite after martensite transformation, *Acta Mater.*, 51(2003), No. 9, p. 2611.

[12] R.L. Miller, Ultrafine-grained microstructures and mechanical properties of alloy steels, *Metall. Mater. Trans. B*, 3(1972), No. 4, p. 905.

[13] H.W. Luo, J. Shi, C. Wang, W.Q. Cao, X.J. Sun, and H. Dong, Experimental and numerical analysis on formation of stable austenite during the intercritical annealing of 5Mn steel, *Acta Mater.*, 59(2011), No. 10, p. 4002.

[14] R.D.K. Misra, V.S.A. Challa, P.K.C. Venkatsurya, Y.F. Shen, M.C. Somani, and L.P. Karjalainen, Interplay between grain structure, deformation mechanisms and austenite stability in phase-reversion-induced nanograined/ultrafine-grained austenitic ferrous alloy, *Acta Mater.*, 84(2015), p. 339.

[15] T. Lee, M. Koyama, K. Tsuzaki, Y.H. Lee, and C.S. Lee, Tensile deformation behavior of Fe–Mn–C TWIP steel with ultrafine elongated grain structure, *Mater. Lett.*, 75(2012), p. 169.

[16] W.H. Zhou, X.L. Wang, P.K.C. Venkatsurya, H. Guo, C.J. Shang, and R.D.K. Misra, Structure–mechanical property relationship in a high strength low carbon alloy steel processed by two-step intercritical annealing and intercritical tempering, *Mater. Sci. Eng. A*, 607(2014), p. 569.

[17] W.H. Zhou, H. Guo, Z.J. Xie, X.M. Wang, and C.J. Shang, High strength low-carbon alloyed steel with good ductility by combining the retained austenite and nano-sized precipitates, *Mater. Sci. Eng. A*, 587(2013), p. 365.

[18] W.H. Zhou, H. Guo, Z.J. Xie, C.J. Shang, and R.D.K. Misra, Copper precipitation and its impact on mechanical properties in a low carbon microalloyed steel processed by a three-step heat treatment, *Mater. Des.*, 63(2014), p. 42.

[19] Z.J. Xie, S.F. Yuan, W.H. Zhou, J.R. Yang, H. Guo, and C.J. Shang, Stabilization of retained austenite by the two-step intercritical heat treatment and its effect on the toughness of a low alloyed steel, *Mater. Des.*, 59(2014), p. 193.

[20] Z.J. Xie, L. Xiong, G. Han, X.L. Wang, and C.J. Shang, Thermal stability of retained austenite and properties of a multi-phase low alloy steel, *Metals*, 8(2018), No. 10, p. 807.

[21] Z.J. Xie, G. Han, W.H. Zhou, C.Y. Zeng, and C.J. Shang, Study of retained austenite and nano-scale precipitation and their effects on properties of a low alloyed multi-phase steel by the two-step intercritical treatment, *Mater. Charact.*, 113(2016), p. 60.

[22] G. Han, Z.J. Xie, L. Xiong, C.J. Shang, and R.D.K. Misra, Evolution of nano-size precipitation and mechanical properties in a high strength-ductility low alloy steel through in-

tercritical treatment, *Mater. Sci. Eng. A*, 705(2017), p. 89.

[23] G. Han, Z.J. Xie, B. Lei, W.Q. Liu, H.H. Zhu, Y. Yan, R.D.K. Misra, and C.J. Shang, Simultaneous enhancement of strength and plasticity by nano B2 clusters and nano-γ phase in a low carbon low alloy steel, *Mater. Sci. Eng. A*, 730(2018), p. 119.

[24] W.J. Nie, X.M. Wang, S.J. Wu, H.L. Guan, and C.J. Shang, Stress-strain behavior of multi-phase high performance structural steel, *Sci. China Technol. Sci.*, 55(2012), No. 7, p. 1791.

[25] J. Shi, X.J. Sun, M.Q. Wang, W.J. Hui, H. Dong, and W.Q. Cao, Enhanced work-hardening behavior and mechanical properties in ultrafine-grained steels with large-fractioned metastable austenite, *Scripta Mater.*, 63(2010), No. 8, p. 815.

[26] Z.J. Xie, C.J. Shang, W.H. Zhou, and B.B. Wu, Effect of retained austenite on ductility and toughness of a low alloyed multi-phase steel, *Acta Metall. Sin.*, 52(2016), No. 2, p. 224.

[27] K.J. Kim and L.H. Schwartz, On the effects of intercritical tempering on the impact energy of Fe–9Ni–0.1C, *Mater. Sci. Eng.*, 33(1978), No. 1, p. 5.

[28] C.A. Pampillo and H.W. Paxton, The effect of reverted austenite on the mechanical properties and toughness of 12 Ni and 18 Ni (200) maraging steels, *Metall. Mater. Trans. B*, 3(1972), No. 11, p. 2895.

[29] S.D. Antolovich and B. Singh, On the toughness increment associated with the austenite to martensite phase transformation in TRIP steels, *Metall. Mater. Trans. B*, 2(1971), No. 8, p. 2135.

[30] W.H. Zhou, Z.J. Xie, H. Guo, and C.J. Shang, Regulation of multi-phase microstructure and mechanical properties in a 700 MPa grade low carbon lowalloy steel with good ductility, *Acta Metall. Sin.*, 51(2015), No. 4, p. 407.

[31] M. Mukherjee, S. Tiwari, and B. Bhattacharya, Evaluation of factors affecting the edge formability of two hot rolled multiphase steels, *Int. J. Miner. Metall. Mater.*, 25(2018), No. 2, p. 199.

[32] C.F. Kuang, Z.W. Zheng, M.L. Wang, Q. Xu, and S.G. Zhan, Effect of hot-dip galvanizing processes on the microstructure and mechanical properties of 600-MPa hot-dip galvanized dual-phase steel, *Int. J. Miner. Metall. Mater.*, 24(2017), No. 12, p. 1379.

[33] Z.J. Xie, Y.P. Fang, G. Han, H. Guo, R.D.K. Misra, and C.J. Shang, Structure–property relationship in a 960 MPa grade ultrahigh strength low carbon niobium–vanadium microalloyed steel: The significance of high frequency induction tempering, *Mater. Sci. Eng. A*, 618(2014), p. 112.

[34] S. Van Der Zwaag, L. Zhao, S.O. Kruijver, and J. Sietsma, Thermal and mechanical stability of retained austenite in aluminum-containing multiphase TRIP steels, *ISIJ Int.*, 42(2002), No. 12, p. 1565.

[35] D.V. Edmonds, K. He, F.C. Rizzo, B.C. De Cooman, D.K. Matlock, and J.G. Speer, Quenching and partitioning martensite—A novel steel heat treatment, *Mater. Sci. Eng. A*, 438-440(2006), p. 25.

[36] C.K. Syn, B. Fultz, and J.W. Morris, Mechanical stability of retained austenite in tempered 9Ni steel, *Metall. Trans. A*, 9(1978), No. 11, p. 1635.

[37] B. Fultz, J.I. Kim, Y.H. Kim, and J.W. Morris, The chemical composition of precipitated austenite in 9Ni steel, *Metall. Trans. A*, 17(1986), No. 6, p. 967.

[38] B. Fultz, J.I. Kim, Y.H. Kim, H.J. Kim, G.O. Fior, and J.W. Morris, The stability of precipitated austenite and the toughness of 9Ni steel, *Metall. Trans. A*, 16(1985), No. 12, p. 2237.

[39] Y.H. Yang, Q.W. Cai, D. Tang, and H.B. Wu, Precipitation and stability of reversed austenite in 9Ni steel, *Int. J. Miner. Metall. Mater.*, 17(2010), No. 5, p. 587.

[40] H.F. Xu, J. Zhao, W.Q. Cao, J. Shi, C.Y. Wang, C. Wang, J. Li, and H. Dong, Heat treatment effects on the microstructure and mechanical properties of a medium manganese steel (0.2C–5Mn), *Mater. Sci. Eng. A*, 532(2012), p. 435.

[41] Y.K. Lee and J. Han, Current opinion in medium manganese steel, *Mater. Sci. Technol.*, 31(2015), No. 7, p. 843.

[42] J. Hu, L.X. Du, W. Xu, J.H. Zhai, Y. Dong, Y.J. Liu, and R.D.K. Misra, Ensuring combination of strength, ductility and toughness in medium-manganese steel through optimization of nano-scale metastable austenite, *Mater. Charact.*, 136(2018), p. 20.

[43] Z.J. Xie, C.J. Shang, S.V. Subramanian, X.P. Ma, and R.D.K. Misra, Atom probe tomography and numerical study of austenite stabilization in a low carbon low alloy steel processed by two-step intercritical heat treatment, *Scripta Mater.*, 137(2017), p. 36.

[44] S. Takaki, K. Fukunaga, J. Syarif, and T. Tsuchiyama, Effect of grain refinement on thermal stability of metastable austenitic steel, *Mater. Trans.*, 45(2004), No. 7, p. 2245.

[45] B.H. Jiang, L.M. Sun, R.C. Li, and T.Y. Hsu, Influence of austenite grain size on γ-ε martensitic transformation temperature in Fe–Mn–Si alloys, *Scripta Metall. Mater.*, 33(1995), No. 1, p. 63.

[46] H.S. Yang and H.K.D.H. Bhadeshia, Austenite grain size and the martensite-start temperature, *Scripta Mater.*, 60(2009), No. 7, p. 493.

[47] E. Jimenez-Melero, N.H. Van Dijk, L. Zhao, J. Sietsma, S.E. Offerman, J.P. Wright, and S. van der Zwaag, Martensitic transformation of individual grains in low-alloyed TRIP steels, *Scripta Mater.*, 56(2007), No. 5, p. 421.

[48] S. Hashimoto, S. Ikeda, K.I. Sugimoto, and S. Miyake, Effects of Nb and Mo addition to 0.2%C–1.5%Si–1.5%Mn steel on mechanical properties of hot rolled TRIP-aided steel sheets, *ISIJ Int.*, 44(2004), No. 9, p. 1590.

[49] J. Heslop and N.J. Petch, The ductile-brittle transition in the fracture of α-iron: II, *Philos. Mag.*, 3(1958), No. 34, p. 1128.

[50] N.J. Petch, The ductile-brittle transition in the fracture of α-iron: I, *Philos. Mag.*, 3(1958), No. 34, p. 1089.

[51] S.D. Antolovich, A. Saxena, and G.R. Chanani, Increased fracture toughness in a 300 grade maraging steel as a result of thermal cycling, *Metall. Trans.*, 5(1974), No. 3, p. 623.

[52] X.L. Gui, K.K. Wang, G.H. Gao, R.D.K. Misra, Z.L. Tan, and B.Z. Bai, Rolling contact fatigue of bainitic rail steels:

The significance of microstructure, *Mater. Sci. Eng. A*, 657(2016), p. 82.

[53] G.H. Gao, B.X. Zhang, C. Cheng, P. Zhao, H. Zhang, and B.Z. Bai, Very high cycle fatigue behaviors of bainite/martensite multiphase steel treated by quenching-partitioning-tempering process, *Int. J. Fatigue*, 92(2016), p. 203.

[54] X.L. Wang, Y.R. Nan, Z.J. Xie, Y.T. Tsai, J.R. Yang, and C.J. Shang, Influence of welding pass on microstructure and toughness in the reheated zone of multi-pass weld metal of 550 MPa offshore engineering steel, *Mater. Sci. Eng. A*, 702(2017), p. 196.

[55] X.L. Wang, L.M. Dong, W.W. Yang, Y. Zhang, X.M. Wang, and C.J. Shang, Effect of Mn. Ni, Mo proportion on microstructure and mechanical properties of weld metal of K65 pipeline steel, *Acta Metall. Sin.*, 52(2016), No. 6, p. 649.

[56] X.L. Wang, Y.T. Tsai, J.R. Yang, Z.Q. Wang, X.C. Li, C.J. Shang, and R.D.K. Misra, Effect of interpass temperature on the microstructure and mechanical properties of multi-pass weld metal in a 550-MPa-grade offshore engineering steel, *Weld. World*, 61(2017), No. 6, p. 1155.

[57] X.L. Wang, C.J. Shang, and X.M. Wang, Characterization of the multi-pass weld metal and the effect of post-weld heat treatment on its microstructure and toughness, [in] *HSLA Steels 2015, Microalloying 2015 & Offshore Engineering Steels 2015*, Hangzhou, 2015, p. 481.

[58] X.L. Wang, X.M. Wang, C.J. Shang, and R.D.K. Misra, Characterization of the multi-pass weld metal and the impact of retained austenite obtained through intercritical heat treatment on low temperature toughness, *Mater. Sci. Eng. A*, 649(2016), p. 282.

[59] L.M. Dong, L. Yang, J. Dai, Y. Zhang, X.L. Wang, and C.J. Shang, Effect of Mn, Ni, Mo contents on microstructure transition and low temperature toughness of weld metal for K65 hot bending pipe, *Acta. Metall. Sin.*, 53(2017), No. 6, p. 657.